

RESEARCH PAPER

MODELING OF CARBIDES COMPOSITION IN WELDED ALLOY SYSTEM Ni-34Cr-4,3W-2,3Mo-1,3Al-1,3Ti-1,3Nb-0,1C

Alexander Anatolyevich Glotka^{1)}, Vadim Efimovich Ol'shanetskii¹⁾*¹⁾ Zaporizhzhia Polytechnic National University, Ukraine, Zaporizhzhia, st. Zhukovskogo, 64, 69063* Corresponding author: glotka-alexander@ukr.net, tel.: +380964275651, Zaporizhzhia Polytechnic National University, Ukraine, Zaporizhzhia, st. Zhukovskogo, 64, 69063

Received: 07.07.2021

Accepted: 12.08.2021

ABSTRACT

Theoretical modeling of thermodynamic processes of precipitation of carbide phases, as well as a practical study of the structure and distribution of chemical elements are studied. Based on an integrated approach for the multicomponent system Ni-34Cr-4,3W-2,3Mo-1,3Al-1,3Ti-1,3Nb-0,1C, new regression models have been obtained that make it possible to adequately predict the chemical composition of carbides from the chemical composition of the alloy. A comparative assessment of the calculation results obtained using regression models and experimental data obtained by X-ray spectroscopy is carried out.

Keywords: weldable nickel-based superalloy, carbides, distribution alloying elements, the temperature of precipitation carbides

INTRODUCTION

One of the main ways to improve the manufacturability of structures, the coefficient of metal utilization, and to reduce the labor intensity and energy consumption of products is the widespread use of welded structures [1-5]. Welding of nickel alloys is associated with serious difficulties caused by their special physicochemical properties, namely, a great tendency to form porosity when welding nickel and nickel alloys. This is because in the molten state nickel-based alloys significantly increase the solubility of gases such as nitrogen, hydrogen, oxygen, and upon crystallization and cooling of the metal, their solubility in the alloy sharply decreases, which leads to the formation of pores [6-11]. There is also a high tendency of the metal to form crystallization cracks. This is due to the formation of low-melting eutectics at the grain boundaries. The most negative influence on the embrittlement of the metal is exerted by carbon, which is released in the form of graphite, and sulphur, which is released in the form of nickel sulphide. When welding nickel and its alloys, it is necessary to increase the groove angle, in comparison with steel welding, since the metal of the weld pool of nickel and nickel alloys is less fluid and melted to a shallower depth of [12-20]. Also, when welding Ni-Cr-based alloys, a refractory chromium oxide film may form, this impedes the formation of a weld. Thus, among the main tasks arising in the welding of nickel and nickel alloys are ensuring reliable protection of the welding zone from atmospheric gases, the use of high-purity welding consumables, as well as deoxidation and degassing of the weld pool [21-25]. The objective of this work is to study the specifics of the influence of alloying elements on the distribution of carbides in the structure, their topology, and morphology, as well as their composition for a multicomponent system such as Ni-34Cr-4,3W-2,3Mo-1,3Al-1,3Ti-1,3Nb-0,1C using the computational prediction method CALPHAD (passive experiment) compared with data obtained by scanning electron microscopy (active experiment).

MATERIAL AND METHODS

Modeling of thermodynamic processes occurring during crystallization (cooling) or heating in the structure of alloys was carried out by the CALPHAD method [26, 27]. Modeling these processes allows for a computational prediction and a comparative assessment of the effect of alloying elements in different types of carbides on their distribution and phase composition in the alloys under study. The calculations were carried out for each investigated composition individually with the step-by-step introduction of a specific alloying element into a fixed composition of a multicomponent system. Depending on the alloying system of the alloy, the results obtained by modeling the crystallization process make it possible to calculate the temperatures and the number of precipitated types of carbides, as well as their chemical composition.

In the multicomponent alloying system (Ni-34Cr-4,3W-2,3Mo-1,3Al-1,3Ti-1,3Nb-0,1C), the range of variation of the elements was chosen based on considerations of the maximum and minimum amount of the element introduced into the superalloys. Thus, for the study were selected carbide-forming elements in the following alloying ranges: carbon (0.02-0.2%); titanium (1-6%); niobium (0.1-4%); molybdenum (1-6%); tungsten (1-16%), chromium (1-35%) by weight.

The alloy crystallization process was simulated from the temperature of the liquid state (1600°C) to room temperature (20°C) with a temperature step of 10°C over the entire range, which made it possible to determine the temperature sequence of phase precipitation during crystallization.

Predictive calculations were carried out based on the initial chemical composition of the alloy with the determination of the most probable precipitation of the amount and type of carbides in the structure, as well as their chemical composition after modeling the crystallization process.

Experimentally, the composition of carbides was determined using a REM-1061 scanning electron microscope with an X-ray

spectral microanalysis system. This method was used to study morphology and chemical composition of precipitated carbides in the alloy structure. The conversion of qualitative values into quantitative analysis was carried out automatically according to the program of the device. The relative error of the method is $\pm 0.1\%$ (by weight). The results of calculations of the type of carbides and their chemical composition were compared with the experimental data obtained using electron microscopy. The obtained dependences have sufficiently high coefficients of determination $R^2 \geq 0.9$ and can be used for predictive calculations of the indicated characteristics with a relative error of $\pm 3.5\%$.

RESULTS AND DISCUSSION

Modeling the precipitation of phases in the process of crystallization of the investigated alloy in the temperature range (1600–20°C) showed that the most probable is the precipitation of the main phases in the following order: γ - solid solution; primary carbides; eutectic $\gamma + \gamma'$; type γ' intermetallic compound based on (Ni₃Al). It is known [28-34] that primary carbides have a high decomposition temperature and well harden alloys at elevated operating temperatures.

It was found that the dependences of the dissolution (precipitation) temperatures of MC carbides and their amount on the carbon content are unchanged, and for carbides of the M₂₃C₆ type have a complex character and are optimally described by the dependences (Table 1), which are shown in Figure 1.

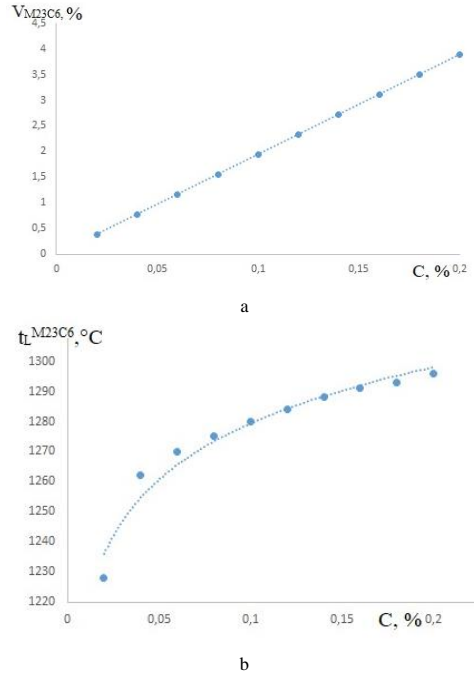


Fig. 1. - Temperature dependences of dissolution (precipitation) of secondary carbides (a); the number of secondary carbides (b) on the carbon content in the alloy

Table 1 - Dependences of the temperature of dissolution (precipitation) of carbides and the content of alloying elements in primary carbides on the content of alloying elements in the alloy

Alloying element	Dissolution (precipitation) temperatures of carbides, °C	The number of carbides (V) and the content of elements in carbide (C), wt%
C	$t_L^{M_{23}C_6}, ^\circ C = 19,452(C) + 0,0033$	$V_{M_{23}C_6} = 26,978 \ln(C) + 1341,5$
Ti	-	$C_{Ti} = -1,3167(C_{Ti} \text{ in alloy})^2 + 15,89(C_{Ti} \text{ in alloy}) + 6,7956$; $C_{Nb} = 1,5658(C_{Ti} \text{ in alloy})^2 - 19,146(C_{Ti} \text{ in alloy}) + 81,708$; $C_W = 0,855(C_{Ti} \text{ in alloy}) + 0,8056$
Nb	$t_L^{MC}, ^\circ C = -4,2143 (C_{Nb}) + 1263,8$	$C_{Nb} = -2,249(C_{Nb} \text{ in alloy})^2 + 18,322(C_{Nb} \text{ in alloy}) + 43,467$; $C_{Ti} = 1,595(C_{Nb} \text{ in alloy})^2 - 13,616 (C_{Nb} \text{ in alloy}) + 36,588$; $C_W = 0,3076(C_{Nb} \text{ in alloy})^2 - 2,1667 (C_{Nb} \text{ in alloy}) + 4,1193$
Cr	$t_L^{M_{23}C_6}, ^\circ C = -0,3746(C_{Cr})^2 + 26,343(C_{Cr}) + 827,2$	$C_{Cr} = -0,0764(C_{Cr} \text{ in alloy})^2 + 4,8775(C_{Cr} \text{ in alloy}) - 4,2879$; $C_{Ni} = 0,0807(C_{Cr} \text{ in alloy})^2 - 4,9991(C_{Cr} \text{ in alloy}) + 80,521$; $C_{Mo} = 0,0143(C_{Cr} \text{ in alloy})^2 - 1,1817(C_{Cr} \text{ in alloy}) + 31,767$; $C_W = -0,0099(C_{Cr} \text{ in alloy})^2 + 0,9073(C_{Cr} \text{ in alloy}) - 9,5687$
Mo	$t_L^{M_{23}C_6}, ^\circ C = -4,9455(C_{Mo}) + 1291,7$	$C_{Mo} = -0,3561(C_{Mo} \text{ in alloy})^2 + 4,2116(C_{Mo} \text{ in alloy}) + 0,8076$; $C_W = 0,3001(C_{Mo} \text{ in alloy})^2 - 3,4499(C_{Mo} \text{ in alloy}) + 15,58$; $C_{Ni} = -0,0576(C_{Mo} \text{ in alloy})^2 + 0,7348(C_{Mo} \text{ in alloy}) + 2,1336$

The change in the temperature of the carbide liquidus for carbides of the MC type is practically not observed when Ti is added to the alloy. However, this leads to a change in the composition of primary carbides and, at a content of more than 4%, to the precipitation of the η -phase (such as Ni-17Ti-4Nb-1Al-0.22Cr). The introduction of more than 2.7% Ti leads to a change in the base of the carbide from niobium to titanium (Fig. 2) (Table 1), while the titanium content in the carbide increases to 55%.

An increase in the concentration of niobium in the alloy leads to a decrease in the temperature of formation (precipitation) of MC carbides (Fig. 3), which is explained by a change in the interatomic bond forces. The formation of primary carbides in this system begins with an Nb concentration of 1%, and its content in the carbide ranges from 60 to 81%. At the same time, the titanium concentration in carbide decreases from 24 to 7% (Table 1).

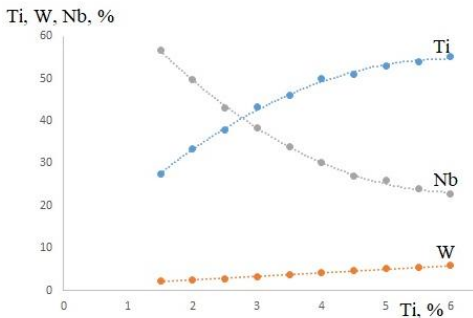


Fig. 2. - Dependences of the amount of titanium, niobium, and tungsten in MC carbides on the titanium content in the alloy composition

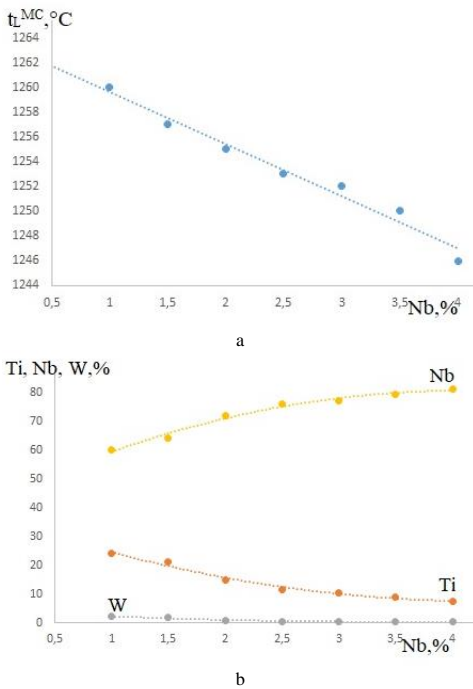


Fig. 3. - Temperature dependence of the dissolution of carbides of the MC type (a) and the amount of titanium, niobium, and tungsten in the MC carbide (b) on the content of niobium in the alloy composition

Chromium is an element that influences the formation of secondary carbides; it has a noticeable effect on the temperature of dissolution (precipitation) of carbides. It was found that the corresponding dependencies (Fig. 4) have a complex character and are described by the following equations (Table 1).

Secondary carbides are formed at a chromium concentration, in this system, at the level of 10%. With an increase in the Cr content in the alloy, the temperature of dissolution (precipitation) of carbides increases, as does its content in the secondary carbide. In this case, the concentration of nickel and molybdenum decreases to 3.5 and 8.8%, respectively, according to parabolic dependences (Table 1). When the concentration of chromium in the alloy is 31%, a solid solution based on Cr is formed, thus chromium ceases to dissolve in nickel.

denum decreases to 3.5 and 8.8%, respectively, according to parabolic dependences (Table 1). When the concentration of chromium in the alloy is 31%, a solid solution based on Cr is formed, thus chromium ceases to dissolve in nickel.

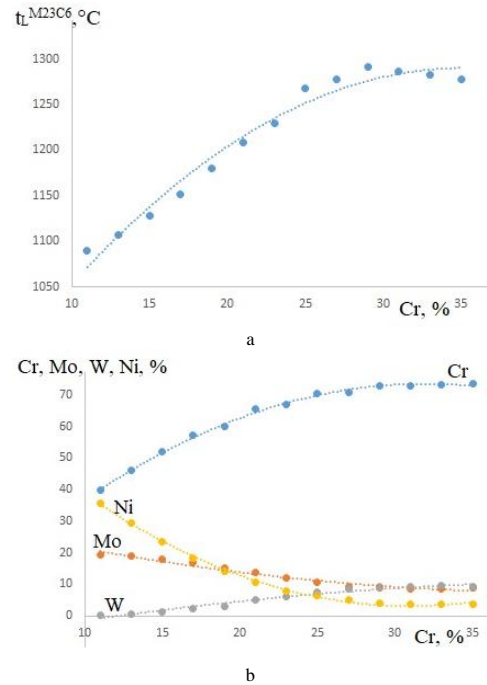
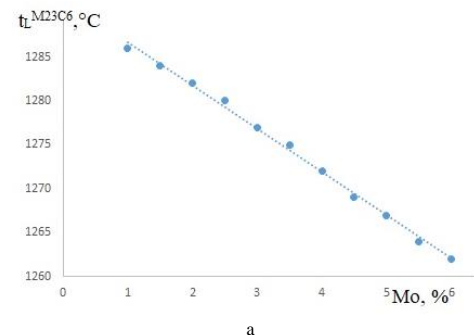


Fig. 4. - Temperature dependence of the dissolution of carbides of the $M_{23}C_6$ type (a); chromium, molybdenum, tungsten, and nickel in $M_{23}C_6$ carbide (b) on the chromium content in the alloy

Figure 5 shows that molybdenum reduces the temperature of dissolution (precipitation) of carbides of the $M_{23}C_6$ type; this nature of the dependence is explained by a change in the forces of interatomic bonds in the secondary carbide. An increase in the content of molybdenum in the alloy does not affect the chromium content in the secondary carbide, it is at the level of 72%. However, the amount of molybdenum in carbide increases to 13%, and tungsten decreases to 5.7% (Fig. 5, b).



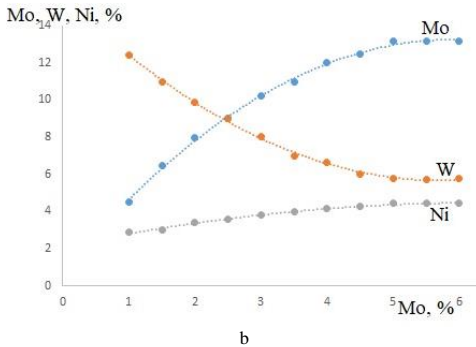


Fig. 5. - Temperature dependence of the dissolution of carbides of the $M_{23}C_6$ type (a); molybdenum, tungsten, and nickel in $M_{23}C_6$ carbide (b) on the content of molybdenum in the alloy composition

Tungsten does not affect the temperature of dissolution (precipitation) of carbides $M_{23}C_6$, it is at the level of 1280°C. An increase in the concentration of tungsten in the alloy leads to a change in the content of alloying elements in the carbides of this system (Fig. 6). Nickel and molybdenum content decrease to 2.7 and 4.4%, respectively, and tungsten content increases to 18% (Table 1).

The results of calculating the phase composition, obtained according to the dependences (Table 1), were further compared with the experimental data obtained using electron microscopy in the microprobe mode on a scanning electron microscope, REM-1061. Typical morphology of primary carbides in the structure of an alloy of this class occurs in the form of separate blocks (Fig. 7). Carbides of the $M_{23}C_6$ type in this alloy are present in a discontinuous block and lamellar forms (Fig. 7).

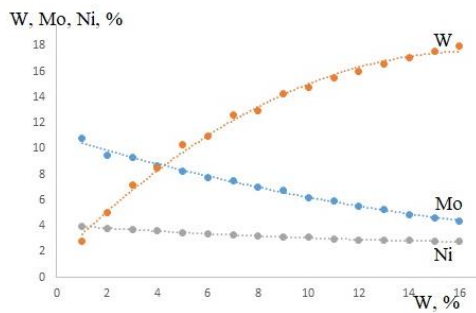


Fig. 6. - Dependences of the content of tungsten, molybdenum, and nickel in carbides of the $M_{23}C_6$ type on the content of tungsten in the alloy composition

The chemical composition of carbides was determined experimentally by X-ray spectral microanalysis, with the help of which the intensity of X-ray radiation was recorded as a function of the energy keV. It was experimentally established that the composition of carbides includes titanium, niobium, tungsten, molybdenum, nickel, and chromium in the following ratios in comparison with the calculated values (Table 2).

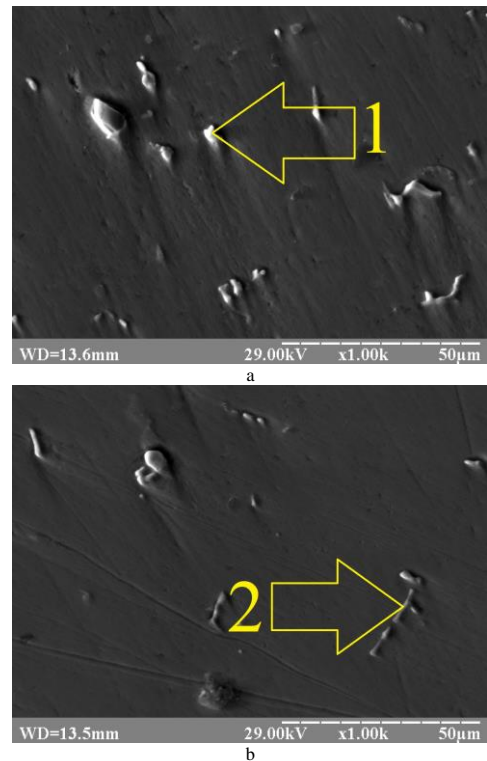


Fig. 7. - Typical morphology of carbides in the alloy structure of the Ni-34Cr-4,3W-2,3Mo-1,3Al-1,3Ti-1,3Nb-0,1C system

Table 2 shows that the calculated and experimental data are in good agreement with each other for almost all elements. Increased content of chromium and nickel is observed in primary and secondary carbides, respectively. Such values can be caused by an increased content of these elements in the alloy. Thus, the calculated data for determining the type and chemical composition of carbides showed good convergence and agreement with the experimental data obtained by electron microscopy.

Table 2 Chemical composition of carbides calculated from the obtained dependences and obtained experimentally by X-ray spectral microanalysis at 20°C

Method of obtaining results	Element content, % wt.						
	Ti	Nb	W	Mo	Ni	Cr	C
Estimated composition MC	25,11	59,09	2,4	-	-	0,49	12,58
Estimated composition $M_{23}C_6$	-	-	9,31	8,62	3,54	73,47	5,06
Experimental composition MC (Fig. 7, point 1)	23,52	51,3	5,76	-	-	6,92	12,5
Experimental composition $M_{23}C_6$ (Fig. 7, point 2)	-	-	8,85	8,86	6,0	71,2	5,05

CONCLUSION

1. Based on an integrated approach for the multicomponent system Ni-34Cr-4,3W-2,3Mo-1,3Al-1,3Ti-1,3Nb-0,1C, new regression models have been obtained that make it possible to adequately predict the chemical composition of carbides by chemical composition alloy. It is shown that the temperature dependences change with the element content and closely correlate with the thermodynamic processes occurring in the system, that is, the curves exhibit extrema accompanying the change in the stoichiometry of carbides or the precipitation of new phases.

2. It was found that with an increase in titanium concentration over 2.7%, the base of MC carbide changes from niobium to titanium, and at 4%, the precipitation of topologically close-packed η -phase. Primary carbides are formed in this system when more than 1% Nb is added. Starting from 10% Cr, secondary carbides are formed in the alloy, and at 31% chromium, the appearance of a solid solution based on chromium is observed, which indicates the termination of its dissolution in nickel.

3. A comparative assessment of the calculated results obtained by regression models and experimental data obtained by the method of X-ray spectroscopy has been carried out. The analysis of the results obtained gave good convergence and can be proposed for predicting the structural components both in industrial alloys and in the development of new materials.

REFERENCES

- A. Sadeghian, S.E. Mirsalehi, F. Arhami: Metall Mater Trans A 52, 2021, 1526–1539.
<https://doi.org/10.1007/s11661-021-06176-x>.
- A. Orozco-Caballero, C. Gutierrez, B. Gan: Journal of Materials Research 2021.
<https://doi.org/10.1557/s43578-021-00133-5>.
- N. Lv, D., Liu Y., Yang: Int J Adv Manuf Technol 112, 2021, 3415–3429.
<https://doi.org/10.1007/s00170-021-06612-7>.
- A. Ota, N. Ueshima, K. Oikawa, S. Imano: *Proceedings of the 9th International Symposium on Superalloy 718 & Derivatives: Energy, Aerospace, and Industrial Applications*. The Minerals, Metals & Materials Series. Springer, Cham.
https://doi.org/10.1007/978-3-319-89480-5_66.
- M. Sedighi, Y. Shajari, S.H. Razavi: Prot Met Phys Chem Surf 57, 2021, 113–120.
<https://doi.org/10.1134/S2070205120060210>.
- D. Liu, X. Cheng, X. Zhang: J. Wuhan Univ. Technol.-Mat. Sci. Edit. 31, 2016, 1368–1376.
<https://doi.org/10.1007/s11595-016-1540-3>.
- P. Kontis, Z. Li, M., Segersäll: Metall Mater Trans A 49, 2018, 4236–4245.
<https://doi.org/10.1007/s11661-018-4709-x>.
- S. Sridar, Y. Zhao, W. Xiong: J. Phase Equilib. Diffus. 2021.
<https://doi.org/10.1007/s11669-021-00871-3>.
- S. Kumar, A.K. Dhingra, S. Kumar: Mech Adv Mater Mod Process 3, 2017, 7.
<https://doi.org/10.1186/s40759-017-0022-4>.
- P.G. Min, V.E. Vadeev, V.A. Kalitsev: Metallurgist 59, 2016, 823–828.
<https://doi.org/10.1007/s11015-016-0179-9>.
- A. Glotka, V. Of'shanetskii: Acta Metallurgica Slovaca 27 (2), 2021, 68–71.
<https://doi.org/10.36547/ams.27.2.813>.
- X. Bai, H. Zhang, G. Wang: Int J Adv Manuf Technol 77, 2015, 717–727.
<https://doi.org/10.1007/s00170-014-6475-2>.
- D. Erdeniz, A.J. Levinson, K.W. Sharp: Metall Mater Trans A 46, 2015, 426–438.
<https://doi.org/10.1007/s11661-014-2602-9>.
- H.W. Jeong, S.M. Seo, B.G. Choi: Met. Mater. Int. 19, 2013, 917–925.
<https://doi.org/10.1007/s12540-013-5003-5>.
- V.I. Titov, N.V. Goundobin, V.N. Kotikov: J Appl Spectrosc 80, 2013, 477–481.
<https://doi.org/10.1007/s10812-013-9791-7>.
- Zh. Gong, Yy. Ma, Hs. Bao: J. Iron Steel Res. Int. 2021.
<https://doi.org/10.1007/s42243-021-00562-w>.
- Z. Jie, J. Zhang, T. Huang: Journal of Materials Research 31, 2016, 3557–3566.
<https://doi.org/10.1557/jmr.2016.383>.
- P. Ritt, O. Lu-Steffes, R. Sakidja: J Therm Spray Tech 22, 2013, 992–1001.
<https://doi.org/10.1007/s11666-013-9947-2>.
- O.A. Glotka: Journal of Achievements in Materials and Manufacturing Engineering 102/1, 2020, 5–15.
<https://doi.org/10.5604/01.3001.0014.6324>.
- A.A. Glotka, S.V. Gaiduk: J Appl Spectrosc 87, 2020, 812–819.
<https://doi.org/10.1007/s10812-020-01075-2>.
- A.S. Shahi, S.S. Sandhu: *Proceedings of the 9th International Symposium on Superalloy 718 & Derivatives: Energy, Aerospace, and Industrial Applications*. The Minerals, Metals & Materials Series. Springer, Cham.
https://doi.org/10.1007/978-3-319-89480-5_59.
- H.M. Tawancy, A.I. Mohammed, L.M. Al-Hadhrami: Oxid Met 84, 2015, 527–539.
<https://doi.org/10.1007/s11085-015-9568-x>.
- A.N. Cherepanov, V.E. Ovcharenko: Phys. Metals Metallogr. 116, 2015, 1279–1284.
<https://doi.org/10.1134/S0031918X1510004X>.
- H. Singh: JOM 67, 2015, 2564–2572.
<https://doi.org/10.1007/s11837-015-1628-9>.
- A.V. Laptev, A.I. Tolochin, D.G. Verbilov: Powder Metall Met Ceram 54, 2015, 416–427.
<https://doi.org/10.1007/s11106-015-9731-6>.
- S.L. Semiatin, J.S. Tiley, F., Zhang: Metall Mater Trans A 52, 2021, 483–499.
<https://doi.org/10.1007/s11661-020-06092-6>.
- S. Sulzer, M. Hasselqvist, H. Murakami: Metall Mater Trans A 51, 2020, 4902–4921.
<https://doi.org/10.1007/s11661-020-05845-7>.
- T. Liang, L. Wang, Y. Liu: J Mater Sci 55, 2020, 13389–13397.
<https://doi.org/10.1007/s10853-020-04931-w>.
- LZ. He, Q. Zheng, XF. Sun, HR. Guan, ZQ. Hu, AK. Tieu, C. Lu, HT. Zhu: Mater Sci Eng A 397(1–2), 2020, 297–304.
<https://doi.org/10.1016/j.msea.2005.02.038>.
- A.A. Glotka, A.N. Moroz: Met Sci Heat Treat 61, 2019, 521–524.
<https://doi.org/10.1007/s11041-019-00456-5>.
- Y.H. Kvasnytska, L.M. Ivaskevych, O.I. Balytskyi: Materials Science, 56 No. 3, 2020, 432–440
<https://doi.org/10.1007/s11003-020-00447-5>.
- A.I. Balyts'kyi, Y.H. Kvasnyts'ka, L.M. Ivas'kevich: Materials Science 54, № 2, 2018, 289–294
<https://doi.org/10.1007/s11003-018-0178-z>.
- V.I. Tkachev, I.M. Levina, L.M. Ivas'kevych: Materials Science 33, No 4, 1997, 524–531.
<https://doi.org/10.1007/BF02537549>.
- A.I. Balitskii, L.M. Ivaskevich: Strength of Materials 50, № 6, 2018, 880–887.
<https://doi.org/10.1007/s11223-019-00035-2>.